

THE 4TH INTERNATIONAL CONFERENCE ON ALUMINUM ALLOYS

COMPETITIVE GROWTH IN QUENCH MODIFIED AND IMPURITY MODIFIED ALUMINUM-SILICON EUTECTICS

R. E. Napolitano, Jr. and T. H. Sanders, Jr.
Georgia Institute of Technology
School of Materials Science & Engineering
Atlanta, Georgia 30332-0245, USA

Abstract

The solidification conditions in Al-Si chill castings were measured for Sr-modified and unmodified eutectics. Spacing-velocity measurements indicated that, at high solidification rates, growth may be described by $\lambda^4 V = \xi G^{-2/3}$ where $\xi = 140$ and $12.3 \mu\text{m}^4 \text{C}^{2/3} \text{s}^{-1} \text{mm}^{1/3}$ for the unmodified and Sr-modified eutectics, respectively. This is in agreement with previously reported results showing a deviation from $\lambda^2 V$ behavior at high growth rates. Specimens solidified at very high rates were also produced with and without Sr additions. TEM investigations showed that, even at rates well in excess of those required for quench modification, the dominant growth mechanism was the twin plane reentrant edge mechanism characteristic of impurity modified growth.

Background

One feature that renders the Al-Si casting alloys particularly useful is their susceptibility to modification. The effect of impurity additions to Al-Si was discovered in 1911 by Frilley¹ when he produced Al-Si with a refined structure from alumina and silica using the Hall process in the presence of Na. This structure was reproduced in 1921 when Pacz² showed that melting Al-Si alloys under a sodium fluoride flux refined or "modified" the eutectic microstructure considerably. Following the work by Pacz, Gayler performed a detailed thermal and metallographic analysis of such alloys during which he showed that the eutectic reaction could be depressed by 10-20°C by this impurity modification and that the eutectic composition could be shifted toward the Si rich side.³ Furthermore, Gayler's results indicated that rapid cooling from the melt as well as sodium addition would result in a similar modification.³ Since the 1920's, much work has been done to characterize the modification transition, and several modifying agents, such as Sr, Sb, Ca, Ce, Pr, Nd, Eu, and La, have been identified. Additionally, both modification methods have been shown to provide significant increases in strength, ductility, and fracture toughness.^{4,5,6,7} The solidification conditions which cause the transition in morphology have been studied in detail.^{8,9,10} It has been shown that the modification by rapid cooling (quench modification) is, in fact, different from modification by the addition of a modifying agent (impurity modification). The resulting morphologies have been shown to exhibit some striking differences indicating the existence of three distinct growth mechanisms.

Normal eutectic growth in Al-Si is characterized by a continuous network of large silicon flakes. The broad faces of the flakes are parallel to the {111} planes of the diamond

cubic Si and there is no preferred orientation relationship with the Al phase.¹¹ Some {111} growth twinning has been observed at low density with twin spacing on the order of 1 micron.¹² An example of the normal eutectic microstructure of Al-Si is shown in Figure 1a.

Quench modified (QM) eutectic growth in Al-Si results in very fine Si particles which have a globular fibrous morphology rather than the flake structure of the normal eutectics. This form of eutectic Si is unfaceted and virtually featureless externally. The particles generally contain a very low density of {111} twins with spacings much larger than the particle dimensions. Some degree of limited branching of the fibrous particles is generally observed while the overall particle growth direction is roughly $\langle 211 \rangle$.¹³ Examples of this structure are provided in Figure 1b.

Impurity modified (IM) eutectic growth results in Si particles which are similar to the quench modified in overall morphology, although typically more fibrous and less globular. The principle growth direction of the fiber or rod shaped particles has been shown to be $\langle 100 \rangle$ with branching in $\langle 211 \rangle$ directions following modification with Na.¹² The impurity modified Si exhibits one dramatic difference when compared to the quench modified variety. Impurity modified Si has been observed to have an extremely high incidence of {111} twinning with twin spacings on the order of 10nm.¹² This extraordinarily high twin density results in a morphology which appears unfaceted but is, in fact, faceted on a very fine scale. Such microfaceting is in sharp contrast to the completely unfaceted quench modified Si. Typical morphological features of impurity modified Si are pictured in Figure 1c.

Quench modified growth is simply the result of high undercooling such that isotropic growth may occur. This has generally been observed at growth rates in excess of 1mm/s. The transition from normal to impurity modified growth, however, involves the mechanism of impurity induced twinning.^{12,13} According to this theory, the adsorption of an impurity atom of an appropriate size initiates a twin. Additionally, this adsorbed atom occupies an intrinsic Si growth site. Normal growth and IM growth can, thus, be differentiated on the basis of the ratio between twin spacing and intrinsic growth ledge spacing.¹² This is illustrated schematically in Figure 2.

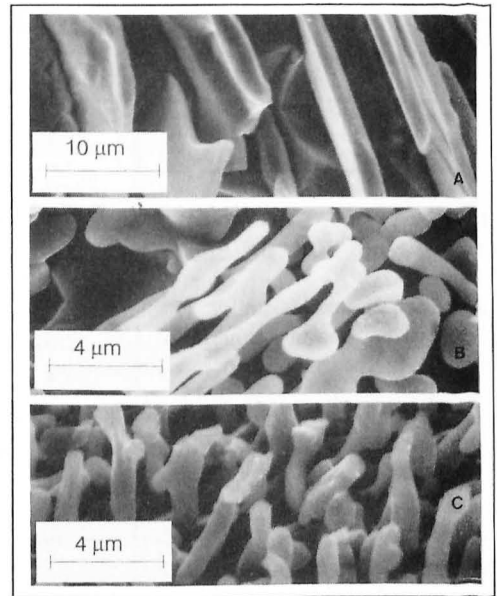


Figure 1. Eutectic structure: (a) Normal; (b) Quench modified; (c) Sr-modified.

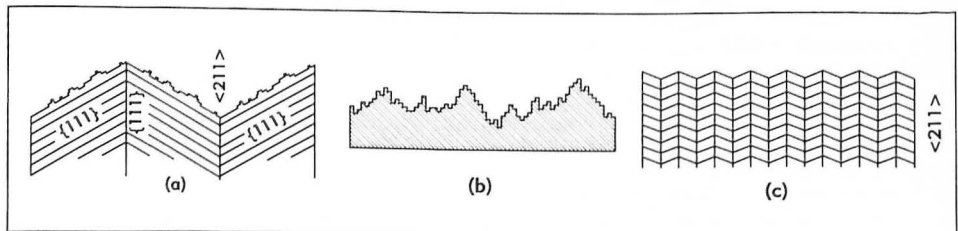


Figure 2. Schematic illustration of (a) Normal; (b) QM; and (c) IM growth modes.²⁸

It was the purpose of this experiment to determine the dominant growth mechanism under conditions which are favorable for both modification transitions. It has been speculated that very high rates of solidification combined with the addition of a modifying agent will result in IM dominant growth.¹³ A second objective was to measure the spacing-velocity relationships resulting from these high rates in the presence of a modifying agent.

Experimental

Casting

Charges of 300g of Al-12Si and Al-12Si-0.1Sr were melted under room air in a graphite crucible. Pouring temperatures of 760°C and 800°C were used. Melts were held at the indicated pouring temperatures for 10 minutes prior to casting. For those castings which were modified with strontium, the additions were made 8 minutes into the 10 minute holding period in the form of an Al-3.4wt%Sr master, allowing 2 minutes for melt homogenization. At the conclusion of the holding period, the alloys were cast into a cylindrical ceramic mold, which was heated to 550°C and situated on a water-cooled copper chill block.

In addition to the chill castings described above, samples of 5 grams were melted and held at 720°C and poured onto the water-cooled chill block, without the ceramic mold. These specimens were termed "splat castings" and were made from Al-12Si and Al-12Si-0.1Sr. Due to the nature of this process, cooling rates could not be quantified but were assumed to be much higher than those in the chill castings.

Specimen Preparation

Specimens for optical metallography were prepared by standard sequential grinding and polishing techniques with a final polish using 0.03 micron SiO₂. Specimens were examined in the unetched condition. SEM specimens were also prepared using standard metallographic techniques followed by a severe etching process which selectively removed the Al matrix while leaving the Si particles intact and in place. This etching process consisted of immersing the specimen in a methanol solution of 5% HNO₃, 3% HCl and 1% HF for 20 minutes at room temperature. TEM specimens were prepared in two ways. Particle extractions were prepared by cutting thin sections from the directional chill castings at the desired axial positions. Each of these thin sections was immersed in the etchant described above for 1-2 hours with ultrasonic agitation for the final five minutes. The specimen was removed from the etchant and the particles were recovered using filter paper which was subsequently immersed in methanol and agitated. Finally, the paper was removed leaving a suspension of Si particles in methanol. Actual TEM specimens were then prepared by placing one drop of this suspension onto a carbon-coated copper grid. Foil specimens were also prepared by sectioning slices of an approximate thickness of 0.5mm from the castings. Slices were then ground to 0.25mm using 600 grit SiC paper. Circular discs were punched from these slices and ground to 0.125mm using 1200 grit SiC paper. The discs were then thinned until perforated by electropolishing with 25% HNO₃ in methanol.

Temperature Profile Measurements

The chill casting setup included a series of seven thermocouples inserted through the ceramic mold at distances of 10, 20, 30, 45, 60, 80, and 100mm from the chill surface. An eighth thermocouple was inserted into an ice bath for reference. During casting, output from each thermocouple was recorded at a frequency of 4hz for the first 20 seconds, 3hz for the following 20 seconds, 2 hz for the next 20 seconds, and 1hz for the remainder of the experiment. The temperature profile data were used to determine the temperature gradient and interface velocity along the length of the casting.

Microscopy

Optical microscopy was used to measure the eutectic spacing, λ , at several locations for each chill casting. This was done by measuring across regularly spaced regions observed on a longitudinal section to obtain a local average. At least ten such measurements were performed and averaged at distances of 15mm, 25mm, 37mm, and 55mm from the chill. A similar technique was used to estimate secondary dendrite arm spacing at various locations as a measure of cooling rate. The eutectic morphology was examined along each chill casting using optical microscopy and SEM. Si particle morphology was characterized for the various solidification conditions using SEM and TEM.

Solidification Conditions

The temperature profile data from the thermocouples inserted in the ceramic mold were smoothed using a five point unweighted average. The velocities of several isotherms were determined by recording the time value at which each thermocouple reached the temperature of interest. The 575°C isotherm was selected as the solid/liquid interface. The 575°C isotherm velocity, thus, represents the solidification rate, V , in the casting. The corresponding temperature gradient, G , ahead of the liquid/solid interface was also estimated from the temperature profile data. This was done by comparing the temperatures of two adjacent thermocouples at the instant in time when the 575°C isotherm passed a particular thermocouple location. Measured values of V and G are plotted in Figure 3. This figure shows that V was roughly constant for the first 50mm while G decreased rapidly with distance from the chill.

Microstructural Measurements

The chill castings were slightly hypoeutectic such that secondary dendrite arm spacing could be measured and correlated to cooling rates using reported data.¹⁴ These cooling rates are plotted in Figure 4. For comparison, this figure also includes cooling rates given by $G \times V$ using the data obtained from measurements described previously. The cooling rates determined by the two methods compare favorably, validating the measurement technique.

The results from the measurement of the eutectic spacing, λ , are plotted in Figure 5, which shows that the eutectic spacing was generally constant

Results

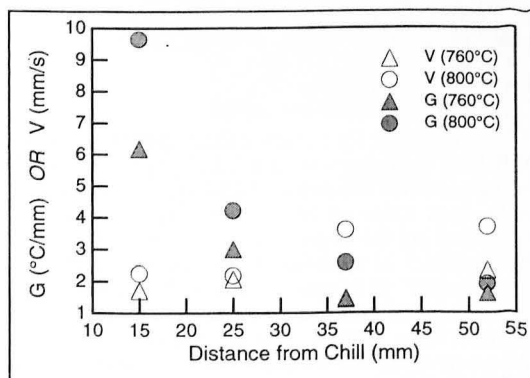


Figure 3. Measured values of G and V .

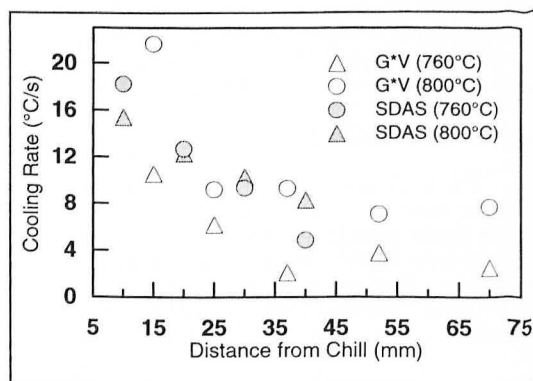


Figure 4. Cooling rate measurements.

throughout the casting. These data also indicate that the eutectic spacing is decreased by the addition of Sr from values near 2 microns to values of approximately 1 micron. There is also a clear effect of pouring temperature on the eutectic spacing with the higher pouring temperature resulting in slightly lower spacings.

Optical microscopy and SEM analysis of the chill castings revealed that the eutectic morphology was constant over the length of the casting, in agreement with the eutectic spacing measurements. The characteristic structures are pictured in Figure 6. This figure also shows that the effect of pouring temperature on the eutectic morphology is

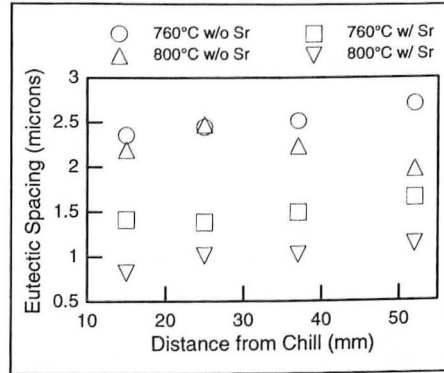


Figure 5. Eutectic spacing measurements.

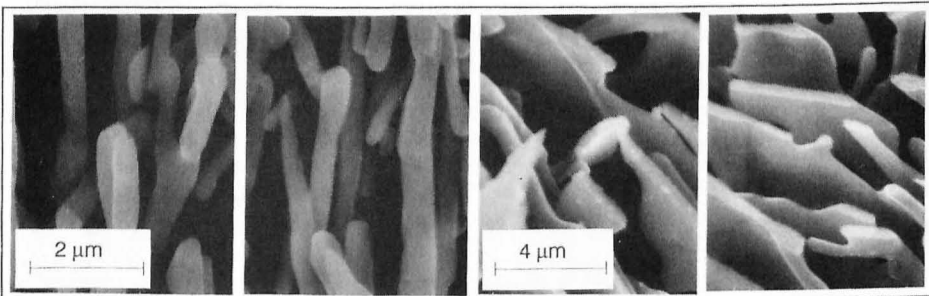
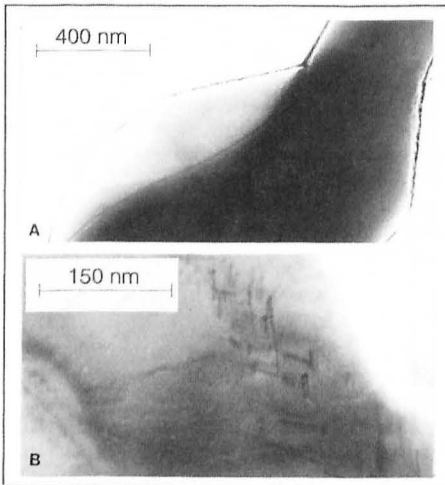


Figure 6. Typical eutectic morphology. (a,b) Sr-modified; (c,d) Unmodified; (a,c) 760°C pour; (b,d) 800°C pour.



very subtle. It is also evident that the Sr-free castings solidified under conditions where "normal" growth was dominant although some evidence of the onset of quench modification does exist.

The TEM investigation revealed that the Sr-free castings exhibited normal growth over the entire casting with a small region of quench modified (QM) Si within 5mm of the chill block. This QM structure is pictured in Figure 7a. The Sr-modified castings exhibited fine twinning, characteristic of impurity modified (IM) growth, throughout the casting, as shown in Figure 7b. The splat castings without Sr contained Si particles which were completely featureless, internally and externally, indicating full quench modification. The Sr-modified splat castings, however, contained Si particles which were heavily twinned on {111} planes indicating that the IM growth mechanism was dominant, as shown in Figure 8.

Discussion

Solidification Conditions

With the results from the interface velocity calculations and the eutectic spacing measurements, the operating conditions of the Al-Si eutectic may be considered. The chill casting data are plotted in Figure 9 for comparison with the reported relationships: $\lambda^2V=382\mu\text{m}^3/\text{s}$ for normal growth and $\lambda^2V=155\mu\text{m}^3/\text{s}$ for Sr-modified growth.^{15,16} The agreement with these relationships is very poor. In fact, the data do not even fall within the limits defined by the extremum condition and the branching limit. It has been shown, however, that there may be a deviation from the λ^2V behavior at high growth rates ($>20\mu\text{m}/\text{s}$) where eutectic solidification may be described by a λ^4V relationship.¹⁵ This deviation is attributed to the nucleation and growth of equiaxed eutectic colonies ahead of the columnar eutectic growth front. Additionally, because the growth of the equiaxed colonies depends geometrically on the primary dendrite spacing, the temperature gradient affects the critical growth rate at which departure from the λ^2V behavior occurs. Reported data have shown the relationship $\lambda^4V=\xi G^{-2/3}$ for hypoeutectic Al-Si, where ξ is a constant.¹⁵ This relationship is plotted in Figure 9, for $\xi=140$ and $12.3\mu\text{m}^4\text{C}^{2/3}\text{s}^{-1}\text{mm}^{1/3}$ and $G=4^\circ\text{C}/\text{mm}$.

Modification Conditions

The tendency for impurity modification to occur can be considered by comparing the required undercooling for normal growth and IM growth, over a range of growth rates as shown in Figure 10. This figure reveals that normal growth should occur at a lower undercooling than IM growth at any velocity or spacing. This would indicate that the impurity modification is an unfavorable growth transition and should never occur. It must, however, be recognized that the normal growth curve in Figure 10 represents normal lamellar growth into a liquid phase which is free from Sr. This, of course, is not an appropriate comparison since the presence of Sr in the melt may have a significant effect on the normal growth of the Si phase. Intrinsic growth sites are occupied by adsorbed Sr atoms rendering the sites inactive for growth by ledge propagation. This ledge pinning or "poisoning" dramatically increases the kinetic undercooling required for normal growth. It is this "poisoned" growth curve which should be compared to the Sr modified growth curve in Figure 10. Such a comparison must show impurity modified growth at lower

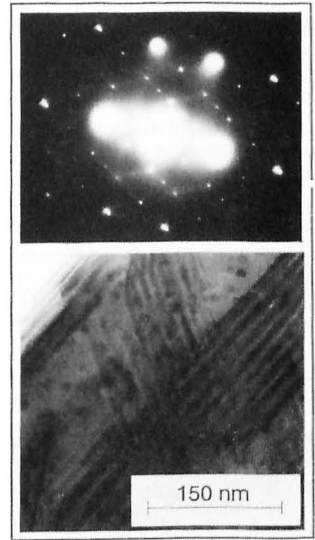


Figure 8. TEM bright field image/SAD pattern pair showing $\{111\}$ twinning in splat cast Sr-modified specimen.

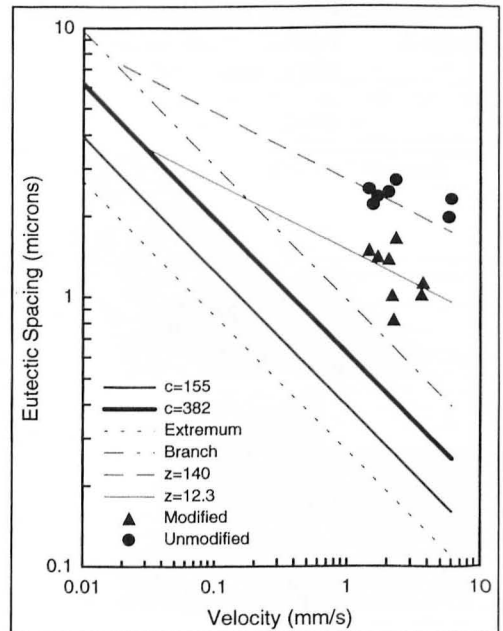


Figure 9. λ - V data from the chill castings.

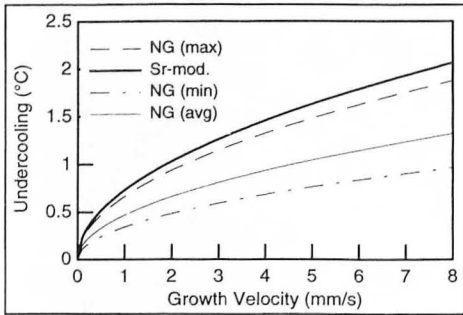


Figure 10. Growth solutions for normal and IM growth, comparing their relative undercoolings.^{17,18}

growth, characteristic of QM, however, requires a much higher kinetic undercooling making this growth mechanism the least favorable. The criterion of a minimum undercooling may not, however, be strictly applicable in this case, since there is no question that QM growth occurs at a much higher total undercooling than the other growth mechanisms. A more appropriate criterion may be a maximum velocity criterion. If an undercooling high enough for any of the three growth mechanisms is assumed, then the mechanism achieving the maximum velocity will dominate. The difference between these two transitions is illustrated by the observation that quench modification may occur in various degrees as shown in Figure 11. This figure illustrates the gradual change in Si morphology with distance from the mold wall in a bulk casting. Near the mold, the undercooling is high enough such that all crystallographic directions can solidify at a rapid rate. As the front advances, undercooling decreases and certain crystallographic directions can no longer keep up. This results in an intermediate growth morphology with some platelike features. Eventually, undercooling is reduced to a value at which the {111} planes are completely inhibited and growth only occurs parallel to these planes. Sr-modification, however, is not a gradual transition. If sufficient Sr is present, complete modification will occur. If insufficient Sr levels are present, then portions of the microstructure may be modified completely while other portions will be completely unmodified. This is referred to as partial modification. The competing processes in this case are growth by intrinsic sites and growth by reentrant twin grooves. The dominant process is, thus, dependent on the number of each type of site, both of which are dependent upon the amount of Sr in the melt. Because of the "double action" of Sr, which poisons intrinsic sites and creates twin sites, the impurity modification transition is extremely sensitive to the amount of Sr added. This explains why intermediate structures are not observed locally. It also explains why the IM transition is more sensitive to some modifying agents than others. Elements which are more likely to be adsorbed and form twins, such as Na, will be less forgiving in terms of the amount required for modification.

Conclusions

At high growth velocities, the growth of the Al-Si eutectic does, indeed, deviate from the $\lambda^2V = \text{constant}$ behavior exhibited at lower rates in favor of a λ^4V relationship, as reported.¹⁵ Furthermore, this deviation occurs in both the unmodified and Sr-modified eutectics. Since the deviation is attributed to the nucleation of equiaxed eutectic colonies, this supports the argument that the primary effect of Sr involves growth rather than nucleation.

The twin plane reentrant edge mechanism (Sr modified growth) is the dominant process at all practical growth rates, even those rates which are high enough to cause quench modification in the normal eutectic, provided that sufficient Sr is present at the growth front.

undercoolings than normal growth. This would indicate that, in the presence of Sr, growth by the twin plane reentrant edge mechanism requires a lower undercooling than the growth of Si by intrinsic ledge propagation, as previously speculated.¹² It is for this reason that eutectic Si exhibits a heavily twinned, microfaceted, fibrous morphology at all practical growth rates, even those which are high enough to cause quench modification. The only criterion for impurity modification, therefore, is sufficient addition of the modifying agent.

Since the morphology of the quench modified eutectic is similar to the impurity modified eutectic, the growth solutions, neglecting kinetic undercooling, will be approximately identical. The isotropic

Sufficient addition of the modifying agent is, thus, the only requirement for the impurity modification growth transition.

The quench modification growth transition occurs at high imposed undercoolings at which isotropic growth is dominant. This transition may be complete or may occur to any intermediate degree. The characterization of the growth conditions corresponding to the different degrees of transition would require quantification of growth velocity as a function of undercooling for all crystallographic directions.

References

1. J. Frilley; Rev. Met., **8** (1911) 457.
2. A. Pacz; U.S. Patent No. 1,387,900 (1921).
3. M.L.V. Gayler; J. Inst. of Metals, **38** (1927) 157.
4. N. Fat-Halla; J. Materials Science, **24** (1989) 2488.
5. N. Fat-Halla; J. Materials Science, **22** (1987) 1013.
6. N. Fat-Halla; J. Materials Science, **25** (1990) 3396.
7. M.F. Haziz, N.K. Fat-Halla, and S.B. Moshref; Z. Metallkunde, **81** (1990) 70.
8. M.D. Hanna, Shu-Zu Lu, and A. Hellawell; Met. Trans., **15A** (1984) 459.
9. H.A.H. Steen and A. Hellawell; Acta Metallurgica, **20** (1971) 363.
10. H.A.H. Steen and A. Hellawell; Acta Metallurgica, **23** (1975) 529.
11. M.G. Day and A. Hellawell; Proc. Royal Society, **A305** (1968) 473.
12. Shu-Zu Lu and A. Hellawell; Met. Trans., **18A** (1987) 1721.
13. Shu-Zu Lu and A Hellawell; J. Crystal Growth, **73** (1985) 316.
14. M.C. Flemings; Solidification Processing, McGraw-Hill, New York, 1974.
15. R. Gruegel and W. Kurz; Met. Trans., **18A** (1987) 1137.
16. B. Toloui and A. Hellawell; Acta Metallurgica, **23** (1975) 529.
17. K.A. Jackson and J.D. Hunt; Trans. TMS-AIME, **236** (1966) 1129.
18. D.J. Fisher and W. Kurz; Acta Metallurgica, **28** (1979) 777.

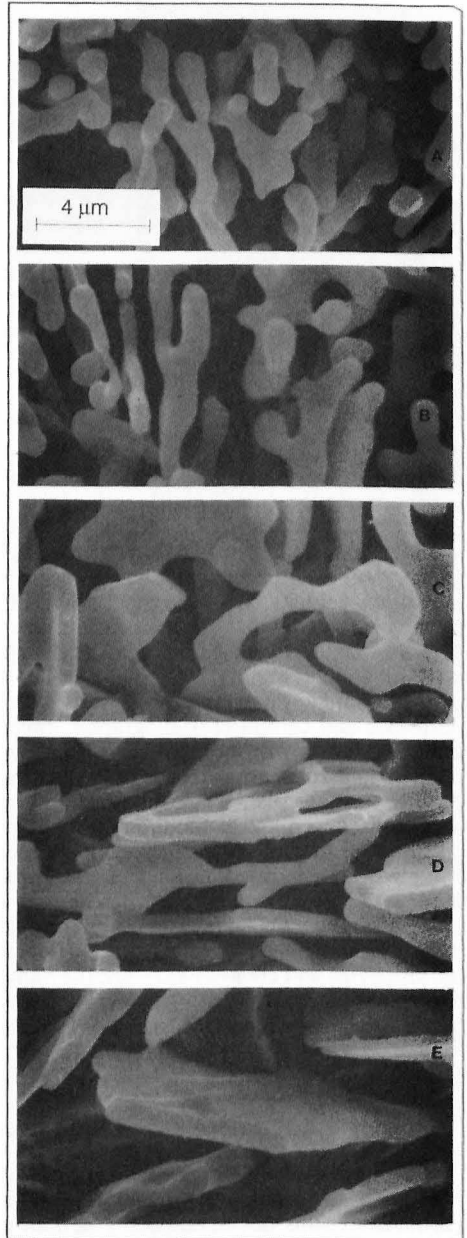


Figure 11. Various degrees of quench modification. Distance from mold wall: (a)5 μ m; (b)100 μ m; (c)250 μ m; (d)500 μ m; (e)800 μ m.